

Negative Feedback Training: A Novel Concept to Improve Robustness of NVCiM DNN Accelerators

Yifan Qin

Computer Science and Engineering
University of Notre Dame
yqin3@nd.edu

Zheyu Yan

Computer Science and Engineering
University of Notre Dame
zyan2@nd.edu

Wujie Wen

Electrical and Computer Engineering
Lehigh University
wuw219@lehigh.edu

Xiaobo Sharon Hu

Computer Science and Engineering
University of Notre Dame
shu@nd.edu

Yiyu Shi

Computer Science and Engineering
University of Notre Dame
yshi4@nd.edu

Abstract—Compute-in-Memory (CiM) utilizing non-volatile memory (NVM) devices presents a highly promising and efficient approach for accelerating deep neural networks (DNNs). By concurrently storing network weights and performing matrix operations within the same crossbar structure, CiM accelerators offer DNN inference acceleration with minimal area requirements and exceptional energy efficiency. However, the stochasticity and intrinsic variations of NVM devices often lead to performance degradation, such as reduced classification accuracy, compared to expected outcomes. Although several methods have been proposed to mitigate device variation and enhance robustness, most of them rely on overall modulation and lack constraints on the training process. Drawing inspiration from the negative feedback mechanism, we introduce a novel training approach that uses a multi-exit mechanism as negative feedback to enhance the performance of DNN models in the presence of device variation. Our negative feedback training method surpasses state-of-the-art techniques by achieving an impressive improvement of up to 12.49% in addressing DNN robustness against device variation.

I. INTRODUCTIONS

In recent times, deep neural networks have brought about a significant transformation in various aspects of our society. Technological advancements, such as ChatGPT [1], transformers [2], and stable diffusion [3], have unveiled unprecedented opportunities in both our professional endeavors and personal lives. However, accelerating deep neural networks for large-scale computing and edge computing is hindered by a critical constraint: frequent data migration between memory chips and computing chips. This constraint arises due to the separation of storage and computation in von Neumann architecture [4]. The von Neumann bottlenecks adversely affect the performance of deep neural network accelerators like GPUs [5]. The traditional approach of enhancing acceleration performance by increasing the number of GPUs becomes impractical for edge devices and leads to concerns regarding latency, energy consumption, as well as environmental and data privacy concerns [6].

The computing-in-memory (CiM) deep neural network (DNN) accelerator [7], utilizing non-volatile memory (NVM) devices, presents a promising solution to address the von

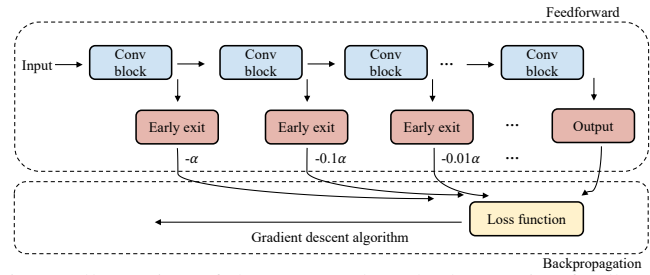


Fig. 1: Illustration of the proposed method: negative feedback training with multi-exit mechanism. Multiple early exits with progressively smaller negative feedback coefficients are introduced to form negative feedback in the loss function.

Neumann bottleneck. CiM accelerators employ the crossbar array structure to store neural network weights and perform matrix calculations in situ, leveraging Kirchhoff's current law. Advanced NVM devices, such as ferroelectric field-effect transistors (FeFETs), resistive random-access memories (RRAMs), magnetoresistive random-access memories (MRAMs), and phase-change memories (PCMs), offer improved memory density and energy efficiency. However, the inherent characteristics of NVM devices, such as cycle-to-cycle (C2C) variation and device-to-device (D2D) variation, result in conductance deviations from the ideal conductance values [8], [9]. Moreover, as these devices undergo aging and frequent read operations, the read disturbance, the lattice relaxation, the accumulation of defects, and other factors may additionally contribute to the deviation in conductance [10]–[13]. Consequently, this leads to the emergence of a Gaussian distribution of device conductance post-writing, thereby adversely affecting the performance of NVCiM DNN accelerators [14].

Numerous approaches have been proposed to address the challenge of device variation. One commonly employed method is the write-verify technique during device programming [8]. This involves applying read pulses after each programming pulse to assess the actual conductance deviation from the target value. Based on this evaluation, fine-tuning programming pulses, either negative or positive, is applied to

adjust the device conductance to the acceptable range around the target level. However, the write-verify operation is energy-intensive and prolongs the programming time, rendering it unsuitable for edge platforms or models with stringent frequency or I/O requirements. In parallel, training methods aim to enhance the robustness of DNNs against perturbations in device conductance is proposed. Neural network architecture search (NAS) [14] explores novel DNN topologies to enhance model robustness, while Bayesian Neural Networks (BNNs) [15] employ variational training techniques to improve robustness. Another promising idea is noise-injection training (or noise-aware training) [16], [17], where random noise, sampled from target conductance distribution, is intentionally introduced into the training process. Specifically, the noise is injected during both the feedforward and gradient calculation stages. Subsequently, the weights without noise are updated through the gradient descent algorithm in the backpropagation. By exposing the DNN to such noise patterns, noise-injection training enhances the network’s noise tolerance and improves the performance of DNN accelerators.

While current research predominantly focuses on optimizing DNNs to enhance robustness, there has been limited attention given to the internal processes and data flow involved in neural network training. Typically, the output of a neural network holds immense significance as it guides the weight updates, thus facilitating the system toward the optimal point. That is to say, output plays a pivotal role in influencing the overall optimization process and positively contributing to its advancement. Nevertheless, the presence of device variations can introduce deviations from the correct path during optimization, potentially causing the model to veer away from the optimal point. Holistic optimization is confronted with a challenge in addressing this situation, as the presence of internal noise can potentially mislead the overall optimization direction, and lead model converge to a suboptimal point or even non-convergence.

To tackle this issue, we draw inspiration from the concept of negative feedback circuits [18] and other control systems that rely on negative feedback theory and propose a novel concept of negative feedback training for DNNs. By incorporating negative contributions from both the output and the network itself, we aim to suppress “noise” in the network optimization process and impose constraints on the internal training process, finally enabling the model’s return to the optimal point.

Specifically, in this paper we show one possible implementation of negative feedback training via multi-exit mechanism [19]–[21], a technique conventionally used to enhance inference efficiency or to reduce energy. In multi-exit DNNs, a series of exits (i.e., early exits) with standard classification layers are added to the DNN backbone to get the intermediate output (e.g., classification prediction). By integrating early exits within the network, the model can swiftly generate predictions at shallower layers, leading to accelerated outcomes for less complex inputs. Each exit functions as a distinct classifier or regressor, helping the network generate multiple outputs simultaneously.

We posit that such a multi-exit mechanism actually offers an avenue to observe and regulate the flow of data within a neural network during training. To clarify, we not trying to enhance the robustness of a multi-exit neural network. Instead, we borrow the multi-exit architecture and apply it as negative feedback mechanism on any neural network during the noise injection training process to enhance the robustness. A conceptual illustration of using multi-exit mechanism for negative feedback training is shown in Figure 1. The negative coefficients on the multiple early exits allow negative feedback to be applied to the network weights update and improve the DNN performance, thereby mitigating the sensitivity and fluctuation of the deep neural network backbone outputs in response to weight variation.

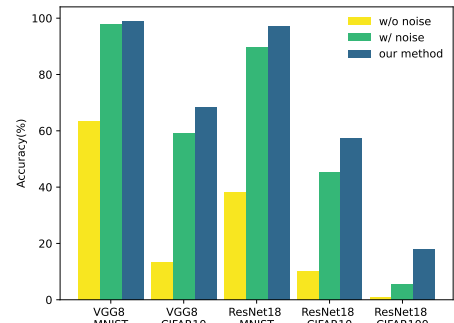


Fig. 2: Comparison of the average accuracy of inference with noise. Models are trained using vanilla DNN training method (train w/o noise), Gaussian noise injection training method, and our negative feedback training method. The data is collected by conducting 200 runs of Monte Carlo simulation based on the device variation model introduced in Section III and IV. Results are presented for five DNN models: VGG-8 on MNIST / CIFAR-10 datasets, and ResNet-18 on MNIST / CIFAR-10 / CIFAR-100 datasets.

Extensive experiments have unequivocally demonstrated that the utilization of negative feedback training surpasses the state-of-the-art (SOTA) baseline performance across various models and datasets, as depicted in Figure 2. Additionally, we conduct simulations to evaluate the efficacy of our approach on NVCiM DNN accelerators across diverse datasets, considering varying Gaussian distributions of device variation. Remarkably, our negative feedback training successfully reduces the impact of device variations. As a result, it mitigates sensitivity and fluctuations of device variation in the DNNs output while enhancing the probability of convergence.

The main contributions are as follows:

- This study proposes the novel concept of negative feedback training for DNNs, aiming to enhance the model’s robustness to device variations.
- We show one possible implementation of negative feedback training, via multi-exit mechanism. Its optimal hyperparameter setting can be easily found within five-step searches.
- In comparison to the conventional noise-injection training method, our approach boosts the model’s convergence

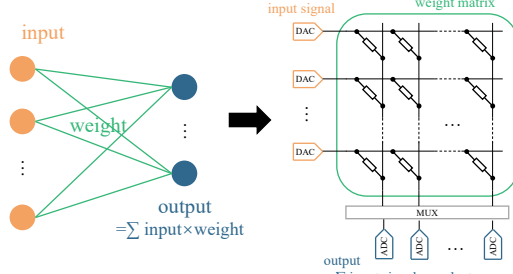


Fig. 3: Illustration of NVM crossbar accelerator of neural network.

probability when confronted with large weight variations.

- Experiments show that our method improves the DNN performance under device variations by up to 1.53%, 9.21%, 7.58%, 11.98%, and 12.49% in VGG-8 for MNIST and CIFAR-10, ResNet-18 for MNIST, CIFAR-10, and CIFAR-100, respectively compared with SOTA baselines.

II. RELATED WORKS

A. Computing-in-memory Crossbar

The compute-in-memory (CiM) represents an innovative approach to overcome the limitations of conventional von Neumann architecture by tightly integrating computation and memory within a crossbar [7]. This paradigm shift enables efficient and high-performance processing by leveraging the inherent parallelism of memory arrays. The working principle of a CiM crossbar is rooted in the utilization of non-volatile memory (NVM) devices, which possess the unique property of exhibiting resistance modulation based on the history of applied voltages. By exploiting this characteristic, CiM crossbars can perform computations directly within the memory array itself, eliminating the need for data movement between separate processing and memory units. As illustrated in Figure 3, the crossbar architecture consists of a dense array of NVM devices organized in rows and columns. Through carefully designed voltage pulses applied to specific rows and columns, the crossbar can perform operations such as matrix multiplications, vector additions, and non-linear transformations in a single clock cycle by a massively parallel manner. This integration of computation and memory at the device level leads to substantial improvements in energy efficiency, latency reduction, and overall system performance, making CiM crossbars a promising avenue for future computing systems.

The performance of NVM based crossbar is susceptible to various forms of variations and noise, including fabrication and inherent device variations [8]. During the manufacturing process, defects in devices or internal wiring can emerge, which may be either localized or global. Furthermore, NVM devices are prone to inherent variations resulting from stochastic fluctuations in the device material. When identical programming pulses are applied multiple times to the same NVM device initialized to its initial conductance state, different conductance values can be obtained. Inherent device variations, unlike those caused by fabrication, are typically independent of the device itself but could still be influenced by the desired

programming target [22]. For the scope of our research, we disregard non-idealities among NVM devices. However, our method can be suitably adapted to accommodate other sources of variations [14], [23].

B. Multi-Exit Neural Networks

Multi-exit neural networks have emerged as an approach to overcome the limitations of single-exit networks, attracting considerable attention in recent years. In contrast to their single-exit counterparts, multi-exit neural networks incorporate multiple branches or pathways within their architecture, enabling predictions to be made at different stages [24]. Each exit serves as an independent classifier or regressor, allowing the network to generate multiple outputs concurrently. By incorporating early exits in the network, the model can quickly make predictions at shallower layers, resulting in faster results for simpler inputs. Conversely, deeper layers with more complex features are utilized for challenging inputs, ensuring higher accuracy.

Multi-exit neural networks operate as a form of multi-objective optimization, where the backbone output and all exits are trained as separate classifiers. The objective is to optimize each output individually, and subsequently compare the computational effort associated with each output, ultimately selecting an optimal result [20], [25]. This trade-off between computational resources and results can be viewed as a variant of ensemble training methods.

C. Device Variation in Accelerators

Several approaches have been proposed to address device variation in NVCiM DNN accelerators, focusing on two main aspects: reducing device variation (hardware) and improving DNN robustness (software).

On the hardware side, device upgrades can be achieved through advancements in material technology and fabrication processes [26]. Additionally, a commonly used technique involves employing write-verify [8] operations during device programming. This approach entails programming the device with a predefined pulse and then reading out the conductance value using a read pulse. The read value is verified to check if it falls within the desired range. If not, additional programming pulses are applied to adjust the device conductance. This iterative read-program process continues until the device conductance aligns with the target conductance range. While effective in reducing deviations in device values, this method is often time-consuming due to the multiple repetitions. Recent research has shown that selectively write-verifying only critical devices can maintain the average accuracy of the DNN, offering a potential efficiency improvement. Furthermore, various circuit designs have been proposed to mitigate the effects of device variation.

On the software side, noise-injection training (or noise-aware training) has emerged as an effective method [16]. This approach introduces variation into DNN weights during the training process, enabling the creation of statistically robust DNN models that can handle device variation. In each training

iteration, a variation instance is sampled from a statistical variations distribution and added to the weights in the feedforward process. During backpropagation, the same noisy weight instance is used for gradient calculations in a deterministic manner. Once the gradient is computed, the variation is cleared, and the noise-free weights are updated based on the gradient. Other software-based approaches involve designing more powerful DNN architectures and employing pruning techniques to enhance DNN robustness [14], [15], [27].

By considering both hardware and software techniques, researchers aim to tackle the challenges posed by device variation in NVCiM DNN accelerators, ultimately improving their performance and reliability.

III. PROPOSED METHOD

In this section, we present a novel approach called “Negative Feedback Training” specifically designed to enhance the performance of DNN accelerators when confronted with device variations. Using the multi-exit mechanism, our method implements negative feedback training by incorporating the outputs of exits as constraints in the backbone training process through the negative feedback coefficients in the loss function. We commence this section by providing a definition of the multi-exit mechanism and outlining our principles for adding exits. Additionally, we delve into the details of negative feedback training utilizing the multiple early exits. Besides, we incorporate noise-injection training by introducing Gaussian distribution noise during training.

A. Multi-Exit Mechanism

Traditionally, multi-exit mechanism based neural networks (or multi-exit neural networks) are trained with a multi-task objective, treating each exit as a separate task that shares the same dataset and labels [19], [25], [28]. Considering the computational operations required for each exit, the model may terminate early at a specific exit to obtain a result that meets the desired accuracy with the fewest possible computational operations. This subsequent comparison of the computational effort associated with each output ultimately facilitates the selection of an optimal result. However, our primary objective in this study is to maximize the robustness and enhance the output performance of the neural network backbone. Essentially, we aim to achieve a single-objective optimization task. Moreover, since the computational requirements are not a concern in our research, the conventional training method for multi-exit neural networks is not relevant to this paper.

Concisely, our method utilizes the multi-exit mechanism as illustrated in Figure 1. This mechanism consists of layered classification structures for each exit positioned at different depths within a DNN model. Each exit operates as an independent probabilistic classifier. *i.e.*, similar to the classification layers in the backbone, each exit maps its input to the probability simplex, which represents a collection of probability distributions over K classes, where K is determined by the

dataset. The exits within the network share a portion of the weights and computations present in the backbone.

The exits closer to the output of the backbone capture more intricate feature information. Choosing the location and number of exits in a DNN involves various principles [29], [30]. In this study, we adopt the semantics principle, treating different types of convolution kernels as distinct functional feature extractors. Consequently, exits are introduced at the end of the respective convolution blocks. Furthermore, to minimize the influence of varying exit sizes on the results, we aim to configure exits with nearly identical parameters. For clarity, Figure 4 and Table I depict the DNN models employed in this study, along with the corresponding exit locations.

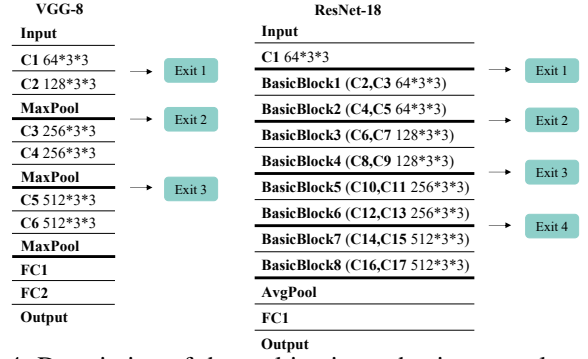


Fig. 4: Description of the multi-exit mechanisms employed in our study: The VGG-8 model incorporates three exit blocks, while the ResNet-18 model utilizes four.

B. Negative Feedback Training

The proposed method utilizes the fundamental principle of classical negative feedback theory. According to this theory, a system, when subjected to external excitation or disturbance, employs negative feedback to suppress or attenuate the disturbance, eventually reaching a new equilibrium state. In our approach, we consider weight variations as a form of “external noise” affecting the system. To enhance the robustness of the system, we aim to suppress this noise through optimization. The biggest challenge then is to identify the negative feedback. Directly using negatively scaled output of a DNN, as in the standard negative feedback system, is not feasible, because it will become a direct scaling of the loss function and will not affect the training process at all. Instead, we need something that can follow the change in the output but is not exactly identical. This leads us to consider the multi-exit mechanism, where the intermediate outputs from early exits provide hints on the final output. By multiplying the outputs from these early exits with negative feedback coefficients and using it as a regularizer in the loss function, as shown in Figure 1 and equation (1), we can effectively enhance the robustness again the “external noise”.

Since the deeper exits of the network handle more complex feature information, we assign smaller negative feedback coefficients to them. This ensures that the impact on the system is reduced as the exits deal with more intricate features. The specific values for the negative feedback coefficients are

determined as follows: the negative feedback coefficient for the first exit output is denoted as α , and the subsequent exits outputs have negative feedback coefficients that decay down the sequence at a decay rate of 0.1, *i.e.*, $0.1\alpha, 0.1^2\alpha\dots$

For a DNN with s exits output, the objective can be expressed as:

$$L = \text{CE} \left[\frac{1}{s+1} (\text{output} - \alpha \sum_{i=1}^s 0.1^{i-1} \cdot \text{out}_i), \text{labels} \right] \quad (1)$$

Here CE means cross-entropy loss function, output denotes the output of the backbone and the out_i means the outputs of exit blocks. In our experiments with extensive datasets and neural network backbones, we find that the optimal value of α can always be found in the following set $\{1, 10^{-1}, 10^{-2}, 10^{-3}, 10^{-4}\}$. As such, a five-step search is sufficient to find the optimal setting.

C. The Effect of Noise-Injection Training

One approach commonly employed to enhance the robustness of DNNs against device variations is noise-aware training, also referred to as noise-injection training [17]. This method involves introducing variations to the weights of the DNN during the training process. In our proposed method, we leverage the noise-injection training technique on both the backbone weights and the exit block weights simultaneously. During each iteration of the training process, we randomly sample an instance of variation from the Gaussian distribution specific to the target device variations. This sampled variation is then added to the weights in the feedforward process. Subsequently, in the backpropagation process, the noisy weights and feature maps are utilized to calculate the weight gradient in a deterministic manner. Following this calculation, the noise is removed, and the weights are updated using the gradient descent algorithm. The algorithmic details pertaining to noise-injection training can be found in Algorithm 1.

Algorithm 1 Training (*model*, *w*, *Dist*, *epochs*, *Dataset*, *lr*)

```

1: // INPUT: DNN topology model, DNN weight w, noise
   distribution Dist, number of training epochs epochs,
   training dataset Dataset, learning rate lr;
2: for  $i = 0$ ;  $i < \text{epochs}$ ;  $i++$  do
3:   for x, labels in Dataset do
4:     Sample  $\Delta w_i$  from Dist;
5:     Apply  $\Delta w_i$  to w of backbone and multi-exit blocks;
6:     Get  $\text{output}$ ,  $\text{out}_1, \text{out}_2 \dots \text{out}_s$  from model(x, w + Δwi);
7:     // output of backbone:  $\text{output}$  and outputs of multi-exit blocks:  $\text{out}_1, \text{out}_2, \dots \text{out}_s$ .
8:     Calculate loss according to eq (1);
9:      $w = w - lr \frac{\partial \text{loss}}{\partial w + \Delta w_i}$ 
10:    // Update w in backbone and multi-exit blocks;
11:    lr = scheduler(lr);
12:  end for
13: end for

```

IV. EXPERIMENTAL EVALUATION

In this section, we present experimental evidence to demonstrate the superiority of our negative feedback training method over existing approaches in improving the robustness of DNN accelerators. Initially, we elaborate on our noise model, which elucidates the relationship between device variation and the noise introduced to the weights during training. Subsequently, we conduct a comparison between our proposed method and the state-of-the-art (SOTA) baseline on different models and multiple datasets. In contrast to the SOTA baseline, we showcase the improvement on inference accuracy with the NVCiM DNN accelerator platform. Moreover, experiments show that our method effectively enhances the probability of model convergence in the presence of large variations.

A. Modeling of Weight Perturbation from Device Variations

In our experimental evaluation, we employ mathematical equations to elucidate the correlation between device variation and weight variation in our modeling approach. Specifically, we examine the influence of device variation occurring during device programming or writing operations on weight variation in DNNs. This pertains to the disparity between the actual conductance of the programmed NVM devices and the desired or target values.

In a computer system, the accurate value is quantized into a binary representation. In the context of DNNs, the weight is typically expressed in terms of a total of M bits. The desired representation of the weight value \mathcal{W}_{ideal} , following the process of quantization, can be articulated as:

$$\mathcal{W}_{ideal} = \frac{\max |\mathcal{W}|}{2^M - 1} \sum_{k=0}^{M-1} i_k \times 2^k \quad (2)$$

where \mathcal{W} represents the value of the floating-point weights and $\max |\mathcal{W}|$ denotes the maximum absolute value among all the weights in the model, and i_k signifies the value of the k^{th} bit of the target weight value.

In the context of NVM devices, certain types such as RRAM exhibit a range of continuous analog conductance states. By carefully modulating these states, it becomes possible to achieve distinct digital conductance levels. Consequently, a NVM device can effectively represent and store N bits of data. Therefore, it becomes possible to represent each weight in a DNN using M/N devices¹. The desired conductance of the j^{th} device, denoted as g_{j_ideal} , can be expressed as follows:

$$g_{j_ideal} = \sum_{k=0}^{N-1} i_{j \times N + k} \times 2^k \quad (3)$$

the negative weights can be mapped in the same manner. Given the previously mentioned variability in device conductance following the programming operation, it is necessary to account for the fluctuations. Therefore, the actual conductance of the device, denoted as g_{j_real} , can be formulated as follows:

¹For the sake of simplicity and generalization, we consider M to be a multiple of N .

$$g_{j_real} = g_{j_ideal} + \Delta g_j \quad (4)$$

where Δg_j is deviation of device conductance.

Now we have the real value of weight after mapping to the NVM device, \mathcal{W}_{real} , shown as:

$$\begin{aligned} \mathcal{W}_{real} &= \frac{\max |\mathcal{W}|}{2^M - 1} \sum_{j=0}^{M/N-1} 2^{j \times N} g_{j_real} \\ &= \mathcal{W}_{ideal} + \frac{\max |\mathcal{W}|}{2^M - 1} \sum_{j=0}^{M/N-1} \Delta g_j \times 2^{j \times N} \end{aligned} \quad (5)$$

In our experimental evaluation, we adopted the findings from previous works [8], [16], [23] as the basis for our parameter settings. We set the value of N to 2, while the value of M was determined by the specific model configuration. In this study, we choose $M = 8$, indicating 8-bit precision for a single DNN weight and 2-bit precision for a single device conductance.

Regarding device variation, we modeled it as a Gaussian distribution denoted by $\Delta g \sim \mathcal{N}(0, \sigma_d)$, where the mean is 0 and the standard deviation is σ_d [31]. Prior research [8] has established that the device parameter σ_d falls within the range of $0 < \sigma_d \leq 0.4$, which depends on device properties and the level of effort invested in programming operations. Techniques such as write-verify with the increased number of read pulses and fine-tuned programming pulses have been shown to enhance device conductance uniformity and reduce σ_d . However, these come at the expense of additional time and energy consumption.

To assess the performance of the proposed method on the NVCiM DNN accelerator, we performed a Monte Carlo simulation. Noise-injection inference was employed, and the average accuracy across these runs was calculated. During the inference process, only the backbone weight of the model was utilized, while the multi-exit blocks were excluded as they do not contribute to the backbone's output. For each inference simulation run, the noise was sampled independently from the same Gaussian distribution used in noise-injection training. Based on the noise-injection training approach, incorporating noise from the distribution of device variation σ_d during the training process enables the model to attain optimal inference outcomes in the presence of such noise. Further details can be found in Algorithm 2.

It is important to note that our model considers device-level optimizations such as write-verify, making this range a generally applicable model for NVM device conductance deviations. Moreover, due to device aging, σ_d may exceed the boundary value of 0.4 [10]–[13]. Nevertheless, our experimental results demonstrate that our approach effectively improves model outputs and enhances convergence probability even in such cases.

B. Experimental Setups

The experiments were conducted within the PyTorch environment using NVIDIA GPUs. Unless otherwise stated,

Algorithm 2 Inference simulation (*model*, *w*, *Dist*(σ_d), *mc*, *Dataset*)

```

1: // INPUT: DNN topology model, DNN weight w, noise
   distribution Dist, device variation  $\sigma_d$ , number of Monte
   Carlo simulation runs mc, test dataset Dataset;
2: train model with noise Dist( $\sigma_d$ ) and save w ;
3: load model with w of backbone;
4: for ( $i = 0$ ;  $i < mc$ ;  $i++$ ) do
5:   sample  $\Delta w_i$  from Dist( $\sigma_d$ );
6:   apply  $\Delta w_i$  to w of backbone;
7:   for x, labels in Dataset do
8:     output = model(x, w +  $\Delta w_i$ );
9:     // output of backbone: output
10:    end for
11:    get accuracy $i$ 
12:  end for
13: Avg.Acc. = avg(accuracy0, accuracy1,  $\dots$ )
```

the reported results represent the average of at least five independent runs. We use the average accuracy of noise-injection inference as the performance metric and we use a Monte Carlo simulation of 200 runs ($mc = 200$). Our experimental findings demonstrate that according to the central limit theorem, conducting 200 simulations results in an average accuracy that falls within a 95% confidence interval of less than $\pm 1\%$. This level of accuracy is considered satisfactory.

In all our experimental evaluations, we consistently set the hyperparameter values as follows: the number of epochs (*epochs*) was fixed at 200. For the CIFAR-10 [32] and CIFAR-100 [32] datasets, we used *start* = 0.1 and *end* = $2 \times \sigma_d$, while for the MNIST dataset [33], we set *start* = 0.2 and *end* = $2 \times \sigma_d$. To explore the impact of the negative feedback coefficient (α), we conducted a search across five different values: 1, 10^{-1} , 10^{-2} , 10^{-3} , 10^{-4} . It is important to note that we maintained other training hyperparameters, including the learning rate, batch size, and learning rate scheduler, in accordance with established best practices for training noise-free models.

C. The Effectiveness of Our Method on MNIST Dataset

This study aims to compare the effectiveness of the negative feedback with multi-exit training method with two baseline approaches: 1) the vanilla training method (train w/o noise) and 2) the Gaussian noise injection training method (train w/ noise) [16]. We have not included a comparison with other optimization methods such as NAS and Bayesian neural networks because we consider them to be orthogonal to our approach, and can be applied in conjunction with our method.

In this section, we present a performance comparison of our method against the two baselines on VGG-8 [34] and ResNet-18 [35] models trained on the MNIST dataset. The architecture diagrams are depicted in Figure 4. The VGG-8 model comprises six convolutional layers (4 types of semantic convolution kernels), and two fully connected layers, so we have three exit block outputs and one backbone output, all of

which are jointly involved in weight updates. The ResNet-18 model consists of 17 convolutional layers (5 types of semantic convolution kernels), and one fully connected layer, so we have four exit block outputs and one backbone output, all outputs jointly involved in weight updates. For clarity, the exit blocks in VGG-8 and ResNet-18 are composed of an average pooling layer followed by two fully connected layers, each with precise parameters as outlined in Table I. We endeavor to equate the parameters of the exit blocks to ascertain the effectiveness of the proposed negative feedback structure in neural network training, independent of the exit block parameters' magnitudes.

TABLE I: Parameters of multi-exit blocks and fully connected layer(s) in VGG-8 and ResNet-18 models.

Blocks and layers	Parameters	
	VGG-8 model	ResNet-18 model
exit 1	2304-512-10/100	2304-512-10/100
exit 2	2048-512-10/100	2304-512-10/100
exit 3	2304-512-10/100	2048-512-10/100
exit 4	-	2304-512-10/100
FC layer(s)	8192-1024-10/100	512-10/100

After five searches for the negative feedback coefficient α in $1, 10^{-1}, 10^{-2}, 10^{-3}, 10^{-4}$, the optimal α for VGG-8 and ResNet-18 models with MNIST dataset are 0.01 and 0.1. Table II illustrates the average accuracy of inference with noise, based on models that are trained using different methods while considering various levels of device conductance variations σ_d . The inference process and variation model follow the approach in Section IV-A, and the vanilla models VGG-8 and ResNet-18 demonstrate remarkable accuracy, reaching 99.65% and 99.61% respectively, in the $\sigma_d = 0.0$ scenario. To evaluate the performance of VGG-8 and ResNet-18 networks on the MNIST classification task, we introduced device variation by setting it up to 0.8, simulating device aging. Within the normal device variation ($\sigma_d \leq 0.4$), negative feedback training resulted in an improvement of up to 1.29% in inference accuracy compared to Gaussian noise injection training, and up to 35.53% compared to no noise injection training for the VGG-8 model. Similar improvements were observed for the ResNet-18 model, with an increase in accuracy of up to 7.58% and 59.14% respectively. When the σ_d value is small, all three methods produced comparable accuracies since σ_d is too small to distinguish them. However, as the σ_d increased, the accuracy of the model trained without noise injection rapidly decayed. In contrast, our method demonstrated greater improvements compared to the noise-injection training.

It is worth noting that when variation exceeds 0.4, the noise-injection training method often failed to yield converged models. Therefore, the reported accuracy of noise-injection training in these cases represents the maximum value (as marked * in Table II) obtained from multiple independent runs rather than the mean.

TABLE II: Comparison of noise inference accuracy with negative feedback training method and baseline methods on MNIST dataset. (*) stands for the maximum accuracy of cases where models easily fail to converge)

Models	Training methods	Device variations σ_d			
		0.2	0.4	0.6	0.8
VGG-8	w/o noise	98.8	63.54	17.61	10.12
	w/ Gaussian noise	99.35	97.77	$\leq 89.56^*$	$\leq 13.71^*$
	our method	99.53	99.30	96.90	70.31
ResNet-18	w/o noise	79.84	38.06	13.17	10.01
	w/ Gaussian noise	98.73	89.62	$\leq 79.95^*$	$\leq 33.18^*$
	our method	97.13	97.20	90.71	77.78

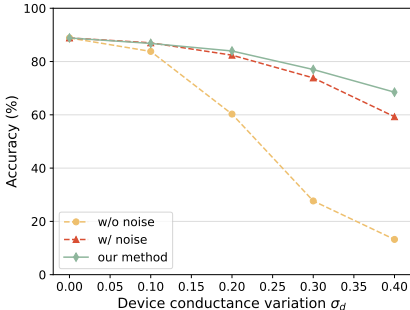
D. The Effectiveness of Our Method on Large Dataset

In the previous section, we demonstrated the effectiveness of negative feedback training in improving the robustness of DNNs using the MNIST dataset. In this section, we extend our experimental evaluation to larger datasets, namely CIFAR-10 and CIFAR-100. Identical network structures are employed as stated in Section IV-C except for the adjustments to the number of output neurons accordingly to the dataset. We investigate the accuracy performance of two different models: VGG-8 on the CIFAR-10 dataset and ResNet-18 on both the CIFAR-10 and CIFAR-100 datasets.

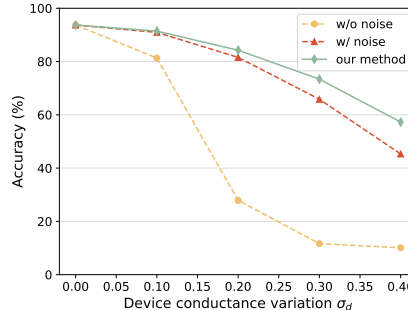
Figure 5 presents the results of our experiments, comparing negative feedback training with the baseline approaches. Remarkably, negative feedback training outperforms the noise injection training baseline for both datasets and models. For the VGG-8 model on CIFAR-10, we found that the optimal value of α is 0.1. Employing negative feedback training resulted in a substantial improvement in the accuracy of inference with noise, reaching up to 9.21%. Similarly, for the ResNet-18 model on CIFAR-10 and CIFAR-100, both the optimal α values are 0.001 and our method improves the accuracy by up to 11.98% and 14.45%, respectively.

E. Increased Convergence Probability of Models

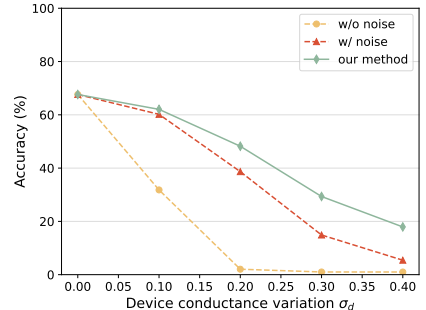
In practical application scenarios of DNN accelerators, the conductance variation of the device σ_d tends to increase over time due to device aging. For instance, multiple read pulses contribute to the accumulation of defects within the RRAM devices, which ultimately results in an amplified device variation [36]. Additionally, in phase-change memory (PCM) devices, as time progresses, lattice relaxation induces conductance drift in the device, and the inconsistent magnitude of device drift also exacerbates the conductance variation [37], [38]. Hence, we conducted experiments on cases where the device conductance approaches or even exceeds the typical threshold of 0.4. The results show that the negative feedback method can effectively improve the convergence probability and accuracy of the model under large device variation compared to the Gaussian noise-injection training baseline. Here we define the concept of model convergence as the occurrence of inference accuracy perturbation within 5% compared with the average accuracy observed across multiple independent runs.



(a) VGG-8 for CIFAR-10



(b) ResNet-18 for CIFAR-10



(c) ResNet-18 for CIFAR-100

Fig. 5: Comparison of noise inference accuracy with negative feedback training method and baseline methods on CIFAR-10 and CIFAR-100 datasets.

In order to ensure that the accuracy of the DNN accelerators falls within an acceptable range, and considering the higher sensitivity of the CIFAR-10 classification task to device variation, we employed σ_d values of 0.6 and 0.4 to models on MNIST and CIFAR-10, respectively. Ten independent runs are conducted with different training methods. The results of unconverged models from these experiments are presented in Table III.

TABLE III: Results of non-converging models in 10 runs: Each value represents the count of models that fail to reach convergence across 10 independent runs.

Training methods	MNIST		CIFAR-10	
	VGG-8	ResNet-18	VGG-8	ResNet-18
w/ Gaussian noise	9	8	1	1
our method	0	0	0	0

In the MNIST classification task, the Gaussian noise-injection training method introduces significant perturbations to the weights. Without negative feedback, both the VGG-8 and ResNet-18 models struggle to handle the noise, resulting in difficulties finding the optimal point and achieving convergence during the training process. Specifically, the accuracy of the VGG-8 models exhibits highly random values distributed between 10% and 60% and only one out of ten runs reaches an optimal accuracy of 89.56%, as shown in Table II. Therefore, it can be concluded that none of the nine runs achieve convergence to the target accuracy. Similarly, eight out of ten ResNet-18 models fail to converge.

In the CIFAR-10 classification task, where the device variation is smaller and has less impact on the weights, the Gaussian noise-injection training also failed to converge in one run for both the VGG-8 and ResNet-18 models.

Throughout all the experiments, our negative feedback training significantly improves the probability of convergence and produces a homogeneous distribution of output accuracy. This improvement can be attributed to the effective suppression of device conductance perturbations by the negative feedback structure during the model training.

F. Synergy with Noise-Injection Training

Here we provide an example of the seamless integration between our negative feedback training method and the noise

injection training method. Table IV presents the noise inference accuracy of VGG-8 and ResNet-18 on CIFAR-10 obtained from applying the negative feedback training with and without the noise injection training method. The table clearly highlights the effective combination of the noise injection training method with the negative feedback method, resulting in a synergistic enhancement of network robustness. Similar observations hold true for other models and datasets and are omitted here in the interest of space.

TABLE IV: Effectiveness of our negative feedback training coupled with noise-injection training on VGG-8 and ResNet-18 models of CIFAR-10 across different σ_d .

Models and methods	Device variation σ_d				
	0.1	0.2	0.3	0.4	
VGG-8	w/o noise injection	84.39	64.16	30.76	14.77
	w/ noise injection	86.80	83.96	77.01	68.50
ResNet-18	w/o noise injection	83.82	34.10	12.50	10.22
	w/ noise injection	91.42	84.25	73.38	57.29

G. Optimal Hyperparameters

Here, we conducted a series of experiments to effectively demonstrate the significance of our multi-exit blocks configuration, including the number of blocks and negative feedback coefficient. With a fixed value of $\sigma_d = 0.4$, we performed three comparative experiments on the VGG-8 model using the MNIST dataset. In each experiment, we selectively removed one exit while keeping the negative feedback coefficients of the remaining exits constant. The results of the noise inference are presented in Table V. It is evident that eliminating any of the exits adversely affects the model's performance. Moreover, when we set the negative feedback coefficients for all exits to be identical, *e.g.*, assigning them the same value as the first exit coefficient (0.01 in this case), the accuracy of noise inference drops to 99.15%, which is once again lower than the model accuracy achieved with our optimal hyperparameter settings. Notably, similar outcomes were observed across different trials on other models and datasets, although those findings are not extensively discussed in this paper.

V. CONCLUSIONS

In this study, we introduced a novel concept of negative feedback training to enhance the robustness of the DNN

TABLE V: Impact of removing exit: We remove one exit in each experiment while maintaining the negative feedback coefficients of the remaining exits constant. Experiments with $\sigma_d = 0.4$ and VGG-8 model on MNIST, trained by negative feedback training.

w/o exit 1	w/o exit 2	w/o exit 3	w/ all exits
99.21	99.16	99.25	99.30

model and optimize its output performance in the presence of device variation. We showed that multi-exit mechanism, conventionally used to reduce latency or enhance energy efficiency of inference, can effectively be used to introduce negative feedback. Experimental results on various neural architectures and datasets show that our proposed method achieved significant improvements over SOTA baselines in terms of both enhancing the robustness of the DNN model and minimizing the likelihood of convergence failure.

REFERENCES

- [1] T. Brown, B. Mann, N. Ryder, M. Subbiah, J. D. Kaplan, P. Dhariwal, A. Neelakantan, P. Shyam, G. Sastry, A. Askell, *et al.*, “Language models are few-shot learners,” *Advances in neural information processing systems*, vol. 33, pp. 1877–1901, 2020.
- [2] A. Vaswani, N. Shazeer, N. Parmar, J. Uszkoreit, L. Jones, A. N. Gomez, Ł. Kaiser, and I. Polosukhin, “Attention is all you need,” *Advances in neural information processing systems*, vol. 30, 2017.
- [3] R. Rombach, A. Blattmann, D. Lorenz, P. Esser, and B. Ommer, “High-resolution image synthesis with latent diffusion models,” in *Proceedings of the IEEE/CVF Conference on Computer Vision and Pattern Recognition*, pp. 10684–10695, 2022.
- [4] Y.-H. Chen, J. Emer, and V. Sze, “Eyeriss: A spatial architecture for energy-efficient dataflow for convolutional neural networks,” *ACM SIGARCH computer architecture news*, vol. 44, no. 3, pp. 367–379, 2016.
- [5] J. D. Owens, M. Houston, D. Luebke, S. Green, J. E. Stone, and J. C. Phillips, “Gpu computing,” *Proceedings of the IEEE*, vol. 96, no. 5, pp. 879–899, 2008.
- [6] Y.-F. Qin, H. Bao, F. Wang, J. Chen, Y. Li, and X.-S. Miao, “Recent progress on memristive convolutional neural networks for edge intelligence,” *Advanced Intelligent Systems*, vol. 2, no. 11, p. 2000114, 2020.
- [7] A. Shafiee, A. Nag, N. Muralimanohar, R. Balasubramonian, J. P. Strachan, M. Hu, R. S. Williams, and V. Srikumar, “Isaac: A convolutional neural network accelerator with in-situ analog arithmetic in crossbars,” *ACM SIGARCH Computer Architecture News*, vol. 44, no. 3, pp. 14–26, 2016.
- [8] W. Shim, J.-s. Seo, and S. Yu, “Two-step write–verify scheme and impact of the read noise in multilevel rram-based inference engine,” *Semiconductor Science and Technology*, vol. 35, no. 11, p. 115026, 2020.
- [9] M. Fritscher, J. Knödtel, M. Mallah, S. Pechmann, E. P.-B. Quesada, T. Rizzi, C. Wenger, and M. Reichenbach, “Mitigating the effects of rram process variation on the accuracy of artificial neural networks,” in *Embedded Computer Systems: Architectures, Modeling, and Simulation: 21st International Conference, SAMOS 2021, Virtual Event, July 4–8, 2021, Proceedings*, pp. 401–417, Springer, 2022.
- [10] M. Rizzi, A. Spessot, P. Fantini, and D. Ielmini, “Role of mechanical stress in the resistance drift of ge2sb2te5 films and phase change memories,” *Applied Physics Letters*, vol. 99, no. 22, p. 223513, 2011.
- [11] J. Y. Raty, W. Zhang, J. Luckas, C. Chen, R. Mazzarello, C. Bichara, and M. Wuttig, “Aging mechanisms in amorphous phase-change materials,” *Nature communications*, vol. 6, no. 1, p. 7467, 2015.
- [12] Y. Chen, H. Lee, P. Chen, P. Gu, C. Chen, W. Lin, W. Liu, Y. Hsu, S. Sheu, P. Chiang, *et al.*, “Highly scalable hafnium oxide memory with improvements of resistive distribution and read disturb immunity,” in *2009 IEEE International Electron Devices Meeting (IEDM)*, pp. 1–4, IEEE, 2009.
- [13] H.-Y. Lee, Y.-S. Chen, P.-S. Chen, P.-Y. Gu, Y.-Y. Hsu, W.-H. Liu, W.-S. Chen, C. H. Tsai, F. Chen, C.-H. Lien, *et al.*, “Comprehensively study of read disturb immunity and optimal read scheme for high speed hfox based rram with a ti layer,” in *Proceedings of 2010 International Symposium on VLSI Technology, System and Application*, pp. 132–133, IEEE, 2010.
- [14] Z. Yan, D.-C. Juan, X. S. Hu, and Y. Shi, “Uncertainty modeling of emerging device based computing-in-memory neural accelerators with application to neural architecture search,” in *2021 26th Asia and South Pacific Design Automation Conference (ASP-DAC)*, pp. 859–864, IEEE, 2021.
- [15] D. Gao, Q. Huang, G. L. Zhang, X. Yin, B. Li, U. Schlichtmann, and C. Zhuo, “Bayesian inference based robust computing on memristor crossbar,” in *2021 58th ACM/IEEE Design Automation Conference (DAC)*, pp. 121–126, IEEE, 2021.
- [16] W. Jiang, Q. Lou, Z. Yan, L. Yang, J. Hu, X. S. Hu, and Y. Shi, “Device-circuit-architecture co-exploration for computing-in-memory neural accelerators,” *IEEE Transactions on Computers*, vol. 70, no. 4, pp. 595–605, 2020.
- [17] X. Yang, C. Wu, M. Li, and Y. Chen, “Tolerating noise effects in processing-in-memory systems for neural networks: A hardware–software codesign perspective,” *Advanced Intelligent Systems*, vol. 4, no. 8, p. 2200029, 2022.
- [18] E. H. Nordholt, *Design of high-performance negative-feedback amplifiers*. Elsevier Scientific Publishing Company Amsterdam, The Netherlands, 1983.
- [19] S. Teerapittayanon, B. McDanel, and H.-T. Kung, “Branchynet: Fast inference via early exiting from deep neural networks,” in *2016 23rd International Conference on Pattern Recognition (ICPR)*, pp. 2464–2469, IEEE, 2016.
- [20] G. Huang, D. Chen, T. Li, F. Wu, L. Van Der Maaten, and K. Q. Weinberger, “Multi-scale dense networks for resource efficient image classification,” *arXiv preprint arXiv:1703.09844*, 2017.
- [21] C. Zhang, M. Ren, and R. Urtasun, “Graph hypernetworks for neural architecture search,” *arXiv preprint arXiv:1810.05749*, 2018.
- [22] B. Feinberg, S. Wang, and E. Ipek, “Making memristive neural network accelerators reliable,” in *2018 IEEE International Symposium on High Performance Computer Architecture (HPCA)*, pp. 52–65, IEEE, 2018.
- [23] Z. Yan, X. S. Hu, and Y. Shi, “Swim: Selective write-verify for computing-in-memory neural accelerators,” in *2022 59th ACM/IEEE Design Automation Conference (DAC)*, IEEE, 2022.
- [24] M. Phuong and C. H. Lampert, “Distillation-based training for multi-exit architectures,” in *Proceedings of the IEEE/CVF international conference on computer vision*, pp. 1355–1364, 2019.
- [25] A. Montanari, M. Sharma, D. Jenkus, M. Aloulah, L. Qendro, and F. Kawsar, “epercpective: energy reactive embedded intelligence for batteryless sensors,” in *Proceedings of the 18th Conference on Embedded Networked Sensor Systems*, pp. 382–394, 2020.
- [26] R. Degraeve, A. Fantini, N. Raghavan, L. Goux, S. Clima, B. Govoreanu, A. Belmonte, D. Linten, and M. Jurczak, “Causes and consequences of the stochastic aspect of filamentary rram,” *Microelectronic Engineering*, vol. 147, pp. 171–175, 2015.
- [27] S. Jin, S. Pei, and Y. Wang, “On improving fault tolerance of memristor crossbar based neural network designs by target sparsifying,” in *2020 Design, Automation & Test in Europe Conference & Exhibition (DATE)*, pp. 91–96, IEEE, 2020.
- [28] Y. Kaya, S. Hong, and T. Dumitras, “Shallow-deep networks: Understanding and mitigating network overthinking,” in *International conference on machine learning*, pp. 3301–3310, PMLR, 2019.
- [29] S. Laskaridis, A. Kouris, and N. D. Lane, “Adaptive inference through early-exit networks: Design, challenges and directions,” in *Proceedings of the 5th International Workshop on Embedded and Mobile Deep Learning*, pp. 1–6, 2021.
- [30] A. Campbell, L. Qendro, P. Liò, and C. Mascolo, “Robust and efficient uncertainty aware biosignal classification via early exit ensembles,” in *ICASSP 2022-2022 IEEE International Conference on Acoustics, Speech and Signal Processing (ICASSP)*, pp. 3998–4002, IEEE, 2022.
- [31] C. Zhou, F. G. Redondo, J. Büchel, I. Boybat, X. T. Comas, S. Nandakumar, S. Das, A. Sebastian, M. Le Gallo, and P. N. Whatmough, “Ml-hw co-design of noise-robust tinyml models and always-on analog compute-in-memory edge accelerator,” *IEEE Micro*, vol. 42, no. 6, pp. 76–87, 2022.
- [32] A. Krizhevsky, G. Hinton, *et al.*, “Learning multiple layers of features from tiny images,” 2009.

- [33] Y. LeCun, L. Bottou, Y. Bengio, and P. Haffner, "Gradient-based learning applied to document recognition," *Proceedings of the IEEE*, vol. 86, no. 11, pp. 2278–2324, 1998.
- [34] K. Simonyan and A. Zisserman, "Very deep convolutional networks for large-scale image recognition," *arXiv preprint arXiv:1409.1556*, 2014.
- [35] K. He, X. Zhang, S. Ren, and J. Sun, "Deep residual learning for image recognition," in *Proceedings of the IEEE conference on computer vision and pattern recognition*, pp. 770–778, 2016.
- [36] C.-Y. Chen, H.-C. Shih, C.-W. Wu, C.-H. Lin, P.-F. Chiu, S.-S. Sheu, and F. T. Chen, "Rram defect modeling and failure analysis based on march test and a novel squeeze-search scheme," *IEEE Transactions on Computers*, vol. 64, no. 1, pp. 180–190, 2014.
- [37] S. Oh, Z. Huang, Y. Shi, and D. Kuzum, "The impact of resistance drift of phase change memory (pcm) synaptic devices on artificial neural network performance," *IEEE Electron Device Letters*, vol. 40, no. 8, pp. 1325–1328, 2019.
- [38] D.-H. Lim, S. Wu, R. Zhao, J.-H. Lee, H. Jeong, and L. Shi, "Spontaneous sparse learning for pcm-based memristor neural networks," *Nature communications*, vol. 12, no. 1, p. 319, 2021.